Eur. Phys. J. Appl. Phys. **31**, 27–30 (2005)
DOI: 10.1051/epjap:2005041

THE EUROPEAN PHYSICAL JOURNAL APPLIED PHYSICS

# Microstructure and morphology evolution in chemical solution deposited semiconductor films: 3. PbSe on GaAs vs. Si substrate

M. Shandalov and Y. Golan[a]

Department of Materials Engineering and the Ilse Katz Center for Nanoscience and Nanotechnology, Ben-Gurion University of the Negev, Beer-Sheva 84105, Israel

Received: 12 December 2004 / Received in final form: 28 February 2005 / Accepted: 4 March 2005
Published online: 21 June 2005 – 

**Abstract.** The microstructure and morphology evolution in nanocrystalline PbSe films chemically deposited on GaAs(100) and GaAs(111) substrates were compared to PbSe films on Si(100) under the same conditions. On GaAs substrates, dense and continuous PbSe films were obtained. We show that the temperature dependent morphological changes on GaAs substrates occurred as a result of increased sample thickness due to higher reaction rates. Notably, the deposition of PbSe on Si(100) did not lead to continuous films and no preferred orientation was observed. The improved wetting between PbSe and GaAs appears to be a key factor responsible for the differences observed on the two substrates.

**PACS.** 68.55.Jk Structure and morphology; thickness; crystalline orientation and texture – 81.07.Bc Nanocrystalline materials – 81.15.Lm Liquid phase epitaxy; deposition from liquid phases (melts, solutions, and surface layers on liquids)

## 1 Introduction

Chemical solution deposition (CD) is an effective and low-cost way to grow high quality nanocrystalline PbSe films without the need for high deposition temperatures, stringent vacuum or plasma generators. CD is particularly advantageous for the synthesis of nanocrystalline semiconductors, in which the energy bandgap, $E_g$, can be adjusted by controlling the grain size of the films due to the quantum size effect. Particular interest in nanocrystalline PbSe is due to its exceptionally large exciton radius ($a_B$) of about 46 nm, following which significant quantum size effects are readily observed in relatively large nanoparticles [1]. Earlier studies on CD of PbSe have been reported, mostly using glass substrates [2–8]. Notably, Gorer and Hodes, investigated the influence of different complexing agents on PbSe deposited on glass and gold substrates [9,10]. Recently, amplified emission from nanocrystalline PbSe was reported, demonstrating the potential of nanocrystalline PbSe material for devices emitting in the technologically useful 1.5 micrometer range [11].

We have reported on chemically deposited PbSe films on GaAs(100) and GaAs(111) substrates [12,13]. Single-phase polycrystalline rocksalt PbSe films were obtained with no evidence for other crystal phases. Transmission electron microscopy (TEM) did not show any evidence for the presence of an amorphous PbSe phase except for an ultrathin interfacial layer, in contrast to reports on the presence of appreciable amounts of amorphous material obtained in different bath compositions [2,4,9,10]. The deposition temperature was found to be an important parameter which strongly influences the film morphology over a surprisingly narrow temperature range. In PbSe films grown on GaAs(100) a gradual transition to strong ⟨111⟩ texture was obtained with increasing deposition temperature, accompanied by a significant increase in crystallite size. In contrast with PbSe deposited on GaAs(100), ⟨111⟩ texture in PbSe on GaAs(111) dominated throughout the deposition temperature range [13]. Following our earlier publications in this series [12,13], this paper describes continued studies on the microstructure and morphology evolution in nanocrystalline PbSe films chemically deposited on various faces of GaAs, and compares the results to deposition on Si(100).

## 2 Experimental

GaAs(100) grown using the *Vertical Gradient Freeze* method was purchased from Wafer Technology Ltd., UK. Silicon(100) grown using the *Czochralski* method was purchased from International Wafer Service Inc., USA. The etch pit density (EPD) for the GaAs(100) was ∼500 etch pits/cm$^2$. This value is comparable to the silicon(100) EPD value (several hundred etch pits/cm$^2$). Film deposition and sample preparation were described in detail previously [13]. TEM and high-resolution TEM (HREM) were carried out using a JEOL 2010 instrument

[a] e-mail: ygolan@bgu.ac.il

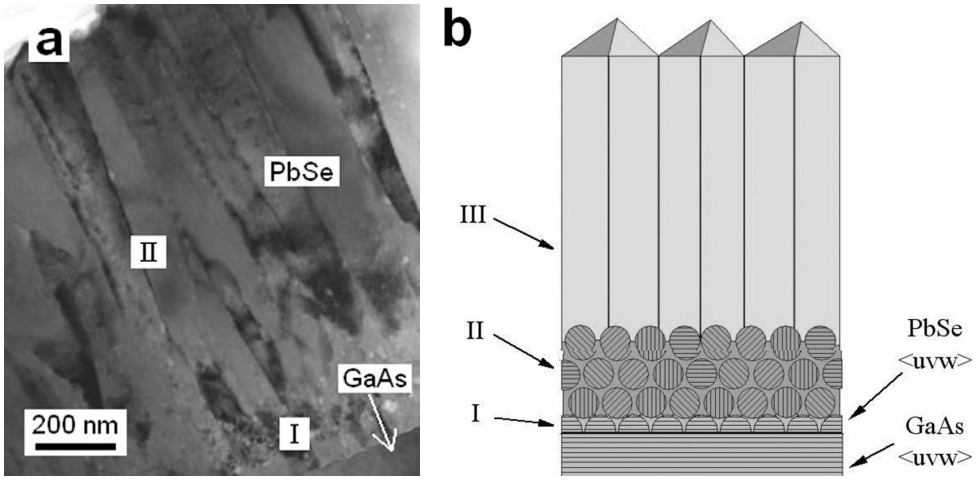


**Fig. 1.** (a) TEM cross-section of PbSe on GaAs showing the two distinct regions present in the film. (b) Schematic illustration showing the morphology evolution in PbSe films on GaAs as a function of thickness. The ⟨u,v,w⟩ indices denote the substrate orientation and the corresponding direction of the PbSe film growth.

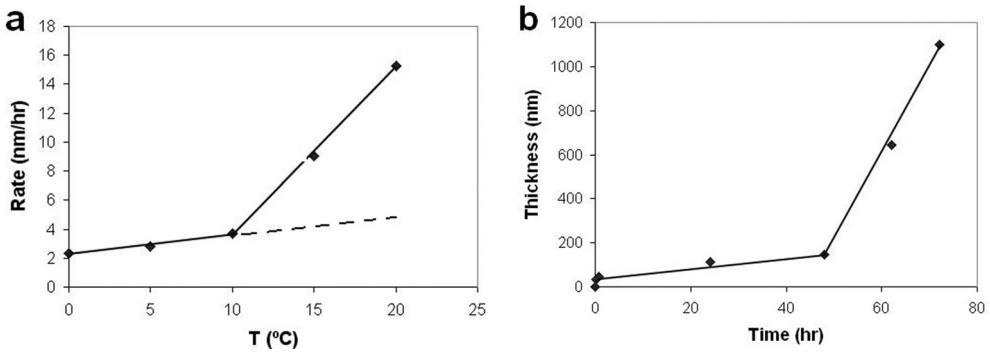


**Fig. 2.** (a) Film growth rate plotted vs. deposition temperature. (b) Film thickness plotted vs. deposition time for constant deposition temperature of 20 °C.

operating at 200 keV. Film thickness was measured from the TEM cross-sections. The Gatan Digital Micrograph 3 software was used for fast Fourier transform (FFT) analysis of HREM lattice images of the PbSe/GaAs interface. Field emission SEM was carried out using an FEI Sirion and JEOL JSM-7400F in Figures 4a, b, respectively.

## 3 Results and discussion

Cross-sectional TEM showed that films deposited at relatively low temperatures (−2 °C to +10 °C, LT) for 72 h on GaAs(100) and GaAs(111) were composed of spherical crystallites (region I in Fig. 1a), while at relatively high temperatures (15 °C, 20 °C, HT) for 72 h, a layer of larger, ⟨111⟩ oriented columnar crystals was observed on top of layer of rounded crystallites (region II in Fig. 1a) [12,13]. Columnar crystals consisted of smaller domains, in agreement with the smaller coherence lengths obtained from X-ray diffraction. Hence three distinct layers can be identified as a function of thickness. (I) First layer of nanocrystals strongly interacting with the substrate. The orientation of these crystallites is governed by the orientation of the underlying GaAs substrate. (II) Subsequent layers of nanocrystals in which ⟨111⟩ texture develops with increasing thickness. (III) Abrupt transition to ⟨111⟩ columnar crystal growth [12,13]. The first layer of crystallites shows epitaxial registry with the GaAs substrate, that disappears in the subsequent layers of crystallites that are not in direct contact with the substrate. The epitaxial relationship is presumably lost in the second layer of nanocrystals due to the greater roughness of the first layer of nanocrystals compared to the GaAs substrate. Such behavior is commonly seen for epitaxial nanocrystals (see for example Ref. [14]). These stages in the morphology evolution of PbSe films on GaAs are schematically illustrated in Figure 1b.

In order to assess the dependence of the deposition rate on temperature, the deposition rate (thickness obtained from TEM cross-sections/deposition time) was plotted vs. $T$ (°C) (Fig. 2a) for PbSe on GaAs(100) for constant deposition time of 72 h. This plot showed two distinct regions with different slopes. From 0 °C to 10 °C the slope of the first part of the linear graph is 0.244 $\mathrm{nm\,h^{-1}\,deg^{-1}}$, then after transition point circa 10 °C the slope significantly increases to 1.16 $\mathrm{nm\,h^{-1}\,deg^{-1}}$. Such behavior can be explained by two different film growth modes. At LT (0–10 °C) the rate of the reaction is very slow. At this

stage, *only* small clusters of PbSe are formed in deposition solution that diffuse towards the surfaces, producing a fine nanocrystalline film. Hence the slope of the first part of the graph indicates the temperature dependence of the formation of the clusters in solution and their diffusion to the surface. At HT (15–20 °C) the greater slope indicates the stronger dependence of the deposition rate with temperature. A dominant microstructural feature in this stage is the ⟨111⟩ oriented growth of large columnar crystals (see layer III in Fig. 1b) which develop on top of the nanocrystalline layer (see layer II in Fig. 1b). Hence, the faster deposition rate at HT reflects a superposition of the deposition rate of layer II (dashed extrapolation line in Fig. 2a) and the deposition rate of the columnar crystals. The thickness (from TEM cross-sections) vs. deposition time plot shown in Fig. 2b for a constant deposition temperature of 20 °C indicates very similar behavior to that seen in the rate vs. temperature plot (Fig. 2a). At the earlier stage of film development (0–48 h), again, *only* small clusters of PbSe are formed in deposition solution and diffuse towards the surfaces. Again, the thickness increases slowly with time. Then at a transition point circa 48 h, columnar growth commences, with a characteristic increase in thickness with deposition time. These results clearly indicate that the temperature-dependent morphological changes in PbSe films chemically deposited on GaAs occur as a function of increased sample thickness due to higher reaction rates. The transition from nanocrystal growth mode to columnar crystal growth mode most probably occurs due to a transition from cluster growth mechanism in the initial stages of growth, to ion-by ion growth, or to coexistence of two parallel mechanisms: cluster *and* ion-by-ion, which has been previously reported to result in large crystals [15]. This time dependent transition from cluster mechanism to ion-by-ion mechanism is expected due to depletion of lead ions in solution (e.g. increase in complexant-to-metal ion concentration ratio) as the reaction proceeds. High complexant concentration leads to reduction of the concentration of free metal ions, which inhibits precipitation of lead hydroxide in form of clusters. Hence, at high complexant concentration the ion-by-ion mechanism is dominant. This transition was confirmed by laser scattering experiments [13], in which a green He-Ne laser beam was transmitted through the deposition solution at high temperature (20 °C) at the final deposition stage and did not show the typical scattering behavior observed from clusters in solution.

We have previously reported on the presence of a thin amorphous layer at the PbSe/GaAs interface [12,13]. This raised an acute question on the mechanism in which the orientation relationship is transmitted across the interface. Recent high resolution TEM (HRTEM) studies provided indications for the presence of intermittent regions of direct contact between crystalline GaAs and crystalline PbSe at the interface, as shown in Figure 3. These regions can serve as nucleation centers for oriented growth, and can therefore explain the epitaxial relationship observed between the first layer of nanocrystals and the substrate. The exact chemical and structural nature of the discontinuous interfacial layer is currently under further investigation.

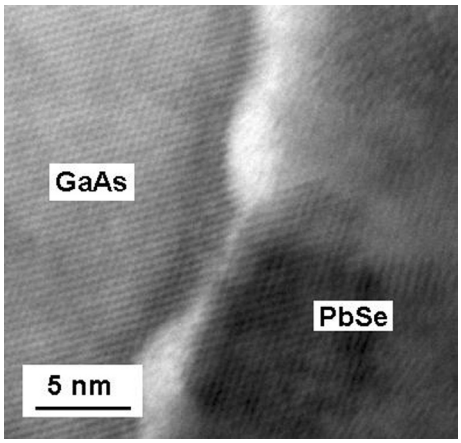


**Fig. 3.** HRTEM cross-sectional image showing an area in which direct contact between GaAs(100) and PbSe is observed.

The continuous and uniform films obtained on GaAs indicated good wetting of the substrate by the PbSe. The good chemical compatibility with GaAs prompted us to test other substrates with different chemical nature. Therefore, the same growth procedure was carried out on Si(100) that were degreased using ethanol prior to deposition. The results clearly showed that PbSe deposited on Si(100) grew significantly slower and resulted in discontinuous layers, in contrast with the compact and uniform films deposited on GaAs substrates. Field emission scanning electron microscopy (FEG-SEM) of PbSe on Si(100) deposited at 0 °C for 3 h showed two types of PbSe crystallites, as shown in Figure 4a: very small crystallites in the order of 10 nm, and about tenfold larger crystallites of 80–100 nm. The crystallites were scattered on the Si surface and did not form a continuous film. Moreover, the image clearly shows a very high contact angle between the PbSe and the GaAs. Note that this image was obtained by strongly tilting the planar sample towards the electron beam. On the other hand, the FEG-SEM image of PbSe on GaAs(100) (Fig. 4b) taken at the same magnification was very different, and showed much more PbSe material present on the surface in the form of a highly continuous nanoparticulate film. TEM cross-sectional images showed the different morphology and microstructure of the PbSe islands at different deposition temperatures (Fig. 5). The film deposited at 0 °C (Fig. 5a) shows islands that are composed of very small PbSe crystallites. The image in Figure 5b deposited at 20 °C shows islands composed of nanocrystalline cores from which larger columnar crystals extend in a fan-like pattern. The overall geometry of this complex structure resembles a box shape, although no evidence has been found for the presence of (100) facets on the surface. HRTEM images of the regions between the islands did not show evidence for the presence of a PbSe wetting layer on the Si substrate. These results confirm the poor wetting properties between PbSe and Si.

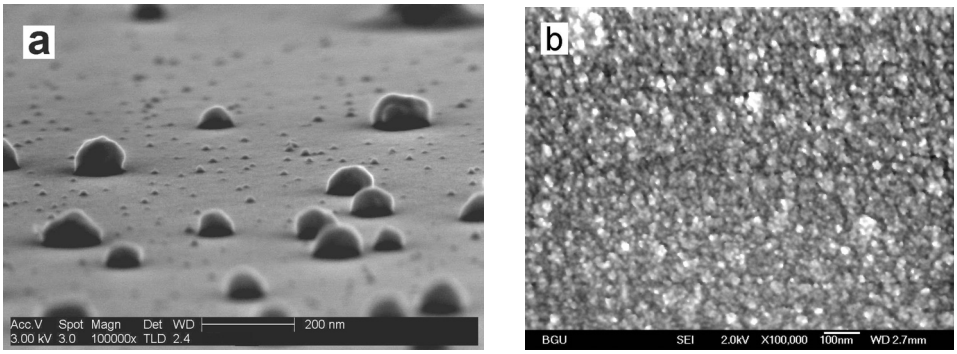


**Fig. 4.** (a) FEG-SEM images of chemically deposited PbSe films deposited on Si(100) substrates. (b) GaAs(100) substrates.

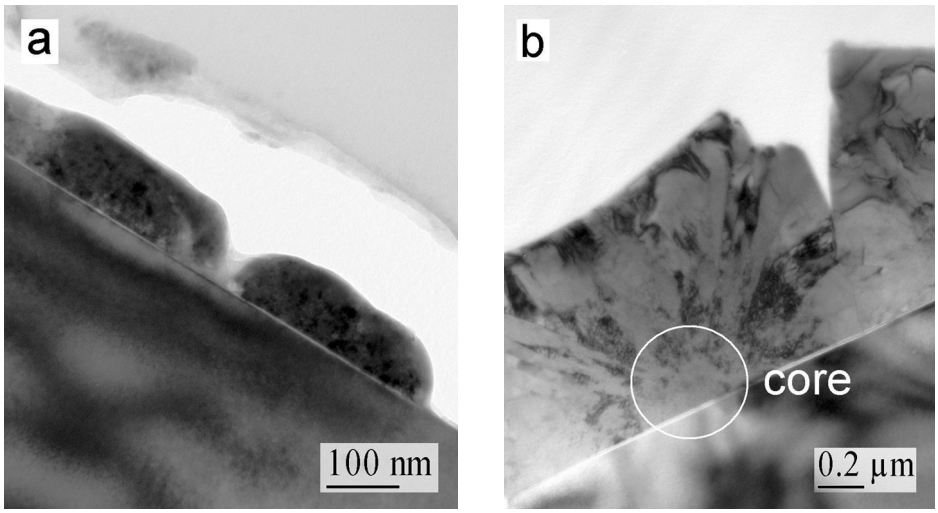


**Fig. 5.** (a) TEM cross-sectional images showing PbSe deposited on Si(100) at a deposition temperature of 0 °C. (b) 20 °C.

## 4 Conclusion

In conclusion, the poor wetting between the PbSe crystallites and Si substrate resulted in discontinuous films of inferior quality. This provides an account for the inferior quality of PbSe films previously deposited on glass or silicon substrates [2–10]. On the other hand, the dense, oriented PbSe films obtained on the various faces of GaAs are a result of the improved chemical compatibility between PbSe and the GaAs substrates.

We thank Vladimir Ezersky for expert assistance in TEM and HREM. The FEG-SEM image in Figure 4a was taken by Ingo Gestmann from Philips Laboratories, and the FEG-SEM image in Figure 4b by Luba Burlaka from BGU. This work was supported by the EU FP-6 STREP project SEMINANO.

## References

1. F. Wise, Acc. Chem. Res. **33**, 773 (2000)
2. I. Grozdanov, M. Najdoski, S.K. Dey, Mater. Lett. **38**, 28 (1999)
3. P. Pramanik, S. Biswas, P.K. Basu, A. Mondal, J. Mater. Sci. Lett. **9**, 1120 (1990)
4. L.P. Biro, R.M. Candea, G. Borodi, A. Darabont, P. Fitori, I. Bratu, D. Dadarlat, Thin Solid Films **165**, 303 (1988)
5. R.C. Kainthla, D.K. Pandya, K.L. Chopra, J. Electrochem. Soc. **127**, 277 (1980)
6. R.M. Candea, N. Dadarlat, R. Turcu, E. Indrea, Phys. Status Solidi A **90**, K91 (1985)
7. G.A. Kitaev, A.Z. Khvorenkova, Russ. J. Appl. Chem. **72**, 1520 (1999)
8. R.N. Mulik, C.B. Rotti, B.M. More, D.S. Sutrave, G.S. Shahane, K.M. Garadkar, L.P. Deshmukh, P.P. Hankare, Indian J. Pure Appl. Phys. **34**, 903 (1996)
9. S. Gorer, A. Albu-Yaron, G. Hodes, Chem. Mater. **7**, 1243 (1995)
10. S. Gorer, A. Albu-Yaron, G. Hodes, J. Phys. Chem. **99**, 16442 (1995)
11. R.D. Schaller, M.A. Petruska, V.I. Klimov, J. Phys. Chem. B **107**, 13765 (2003)
12. M. Shandalov, Y. Golan, Eur. Phys. J. Appl. Phys. **24**, 13 (2003)
13. M. Shandalov, Y. Golan, Eur. Phys. J. Appl. Phys. **28**, 51 (2004)
14. Y. Golan, B. Alperson, J.L. Hutchison, G. Hodes, I. Rubinstein, Adv. Mater. **9**, 236 (1997)
15. G. Hodes, *Chemical Solution Deposition of Semiconductor Films* (Marcel Dekker Inc., New-York-Basel, 2002)